Spreading of cobalt phase and silicate formation in Co/SiO_2 model catalyst

D. Potoczna-Petru * and L. Krajczyk

Institute of Low Temperature and Structure Research, Polish Academy of Sciences, PO Box 1410, 50-950 Wrocław 2, Poland

Received 25 September 2002; accepted 11 January 2003

The electron microscopy technique was used to characterize the cobalt–silica interaction in a model catalyst at high temperature in air. The samples were in the form of thin cobalt films (1 and 4 nm thick) supported on an amorphous layer of SiO_2. It was concluded that cobalt loading determines the evolution of the microstructure, morphology and phase composition. The spreading of the cobalt oxide phase and formation of cobalt silicate was established.

KEY WORDS: Co model catalyst; silicate; Co spreading; TEM; HRTEM.

1. Introduction

Cobalt supported on silica has received great attention due to its application in Fischer–Tropsch (FT) synthesis (high-molecular-weight hydrocarbon formation). Although silica is usually considered as an inert catalytic support, the interaction of cobalt phase with silica and the formation of surface cobalt silicate or silicate-like species during the preparation of Co/SiO_2 has been reported [1–13]. Previous studies showed that the presence of these phases could have a significant effect on the reduction properties and reactivity of the catalyst [1–10,12,13]. As is known, the metallic phase in Co/SiO_2 catalyst is the active form for most applications. Formation of silicates decreases the reducibility of the catalyst under industrially favored conditions and thus reduces the surface area of the active metallic phase. However, Coulter and Sault [7] reported that a certain amount of cobalt silicates in Co/SiO_2 catalyst maximizes the area of reducible cobalt surface available for the FT reaction. As was shown by Steen *et al*. [9] the tendency for formation of silicates increases with increasing surface area of the support, high pH of the impregnation solution and low drying/calcination temperature. According to Puskas *et al*. [5] a Co precipitated catalyst supported on high-surface-area silica was inactive in hydrocarbon synthesis, which could be explained by cobalt silicate formation. Haddad and Goodwin [8] found that water impregnation followed by drying of a reduced and passivated Co/SiO_2 catalyst results in the conversion of sizable amounts of Co phase into silicate/hydrosilicate which are inactive in ethane hydrogenolysis. Work with Co/SiO_2 catalysts in our laboratory indicated the formation of cobalt silicate after calcination at high temperature [11]. The activity of the catalysts was tested by hydrogenation of benzene under conditions when the silicate was formed and after their reduction with hydrogen at high temperature. In both cases the catalysts were inactive [14]. According to Ming and Baker [6] the reducibility of the catalysts is a necessary but not sufficient characteristic in ensuring good activity.

We suppose that besides the chemistry of cobalt, the microstructure and morphology of the formed phase influence the activity of the catalyst. However, little information has been reported on the microstructure of silicate phases [5,8,11]. Puskas *et al*. [5] observed that cobalt silicates often appeared as filamentous structures leaving a significant area of the silica support completely intact. They found that the morphology of silicates in Co/SiO_2 catalysts has an influence on their reduction. The presence of crystalline thin flakes of cobalt silicate lying on an amorphous support was observed in high-resolution transmission electron microscopy (HRTEM) images after calcination of cobalt nitrate precursor supported on SiO_2 in argon at high temperature [11].

The present work was undertaken in order to investigate in more detail the microstructure and morphology evolution of a model Co/SiO_2 catalyst under conditions when the formation of a new phase was reported in real catalysts [6,9,11].

2. Experimental

Silica-supported cobalt model catalysts were obtained by evaporation of thin cobalt films in an Edwards vacuum evaporator onto platinum microscope grids covered with an amorphous, 10–30 nm thick layer of SiO_2. The procedure for SiO_2 film preparation was as

* To whom correspondence should be addressed.

1011-372X/03/0400-0051/0

reported previously [15]. Two different cobalt films with nominal thickness of 1 and 4 nm were prepared. The Co/SiO_2 samples were subjected to thermal treatment in static air at 1073, 1173 or 1273 K for 2 h and then were reduced in purified, flowing hydrogen at 573 K for 4 h. After each stage of the thermal procedure, changes in morphology, structure and composition were monitored using transmission electron microscopy (TEM), HRTEM and selected area electron diffraction (SAED). All the studies were performed using a Philips CM 20 Super Twin microscope.

3. Results

3.1. The 1 nm thick Co/SiO_2 sample

Figure 1 shows a set of TEM images and SAED patterns (insets) of 1 nm Co/SiO_2 after heating in air at 1073, 1173 and 1273 K for 2 h. It is seen that after heating at 1073 K separated, well-defined Co_3O_4 particles with an average size of 9.7 nm appeared (figure 1(a)). Most of them have polyhedron shapes in projection. Heating at 1173 K led to a drastic decrease of the particle size (average particle size of 6.5 nm) with simultaneous change in shape to a rounded one as can be seen in figure 1(b). However, the number of crystallites remained almost the same as in the sample heated at 1073 K. Some broadening of Co_3O_4 rings in the SAED pattern (inset of figure 1(b)) occurred. Additional heat treatment at 1273 K resulted in the disappearance of the particles and only uniform contrast was observed in the micrographs (figure 1(c)). In the SAED pattern only weak, diffuse rings were observed, which could be assigned to amorphous, CoO-like phase.

From these results it appears that the amount of crystalline cobalt phase visible in the TEM images decreases after heating at 1173 K and this phase disappears completely after heating at 1273 K in air.

In the next stage of experiment the samples were subjected to reduction under mild conditions (573 K in H_2 for 4 h) and the TEM images with SAED patterns (insets) are shown in figure 2. As can be seen from figure 2(a), hydrogen treatment of the sample previously oxidized at 1073 K in air caused splitting of the crystallites into smaller particles with an average size of 5.8 nm. The outline of the aggregates formed often preserved the shape of the initial oxide particles (e.g. triangular). The rings in the SAED pattern correspond to f.c.c. Co with the strongest ring originating from (111) planes. The formation of small irregular particles with an average size of 3.1 nm and increased density of

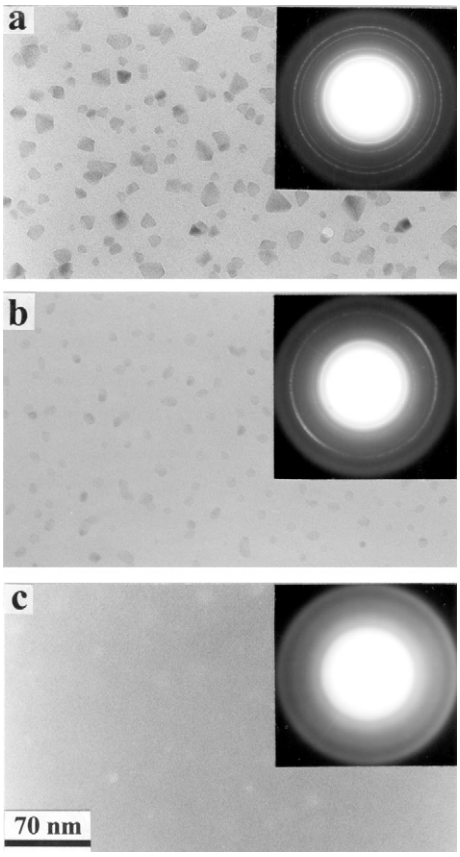

Figure 1. Series of TEM images and SAED patterns (insets) of 1 nm Co/SiO_2 after heating in air for 2 h at: (a) 1073, (b) 1173 and (c) 1273 K.

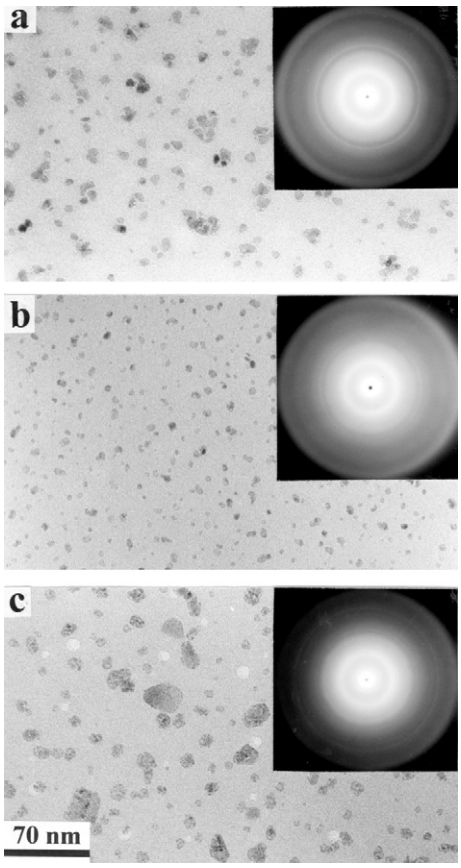

Figure 2. Series of TEM images and SAED patterns (insets) of 1 nm Co/SiO_2 after heating in hydrogen (573 K, 4 h) following previous oxidation in air for 2 h at: (a) 1073, (b) 1173 and (c) 1273 K.

particles was observed after heating at 573 K in hydrogen the sample oxidized at 1173 K (figure 2(b)). For the sample oxidized at 1273 K in air, reduction caused the reappearance of the crystalline phase (figure 2(c)) in the form of porous aggregates with an average size of 8.7 nm. In both cases broad rings in the SAED patterns could not be unequivocally identified; however, they may be ascribed as Co-like and CO_2SiO_4-like, respectively.

3.2. *The 4 nm thick Co/SiO_2 sample*

The series of TEM images and SAED patterns (insets) of samples with 4 nm initial thickness of cobalt, after heating at 1073, 1173 and 1273 K in air, is shown in figure 3. As can be seen, the heating caused sintering of the cobalt phase and two populations of particles are present on the support: larger, well-formed crystallites and smaller ones with size less than 10 nm and nearly circular outline (figure 3). The small particles are situated not only on the SiO_2 substrate but also on the larger cobalt oxide particles. In the micrographs of the sample heated at 1273 K specific regions with different morphology and contrast appear (figure 3(c)). While the average size of crystallites in the specific region was 23.0 nm, in typical regions it was 14.8 nm. In the SAED patterns of the samples continuous rings corresponding to Co_3O_4 (JCPDF file 9-418) were observed. Moreover, additional spots occurred in the samples heated at 1173 and 1273 K (insets of figures 3(b) and (c)). These spots, corresponding, among others, to interplanar spacings of 0.51, 0.37 and 0.35 nm, could not be assigned to any metallic or oxidized phase of cobalt or to any crystalline form of silica. However, the reflection particularly well visible for the sample heated at 1273 K (figure 3(c)) may be ascribed to cobalt orthosilicate (JCPDF file 15-865).

The experiments with mild reduction at 573 K of the oxidized samples gave additional information about the microstructure of the formed phases (figure 4). In all

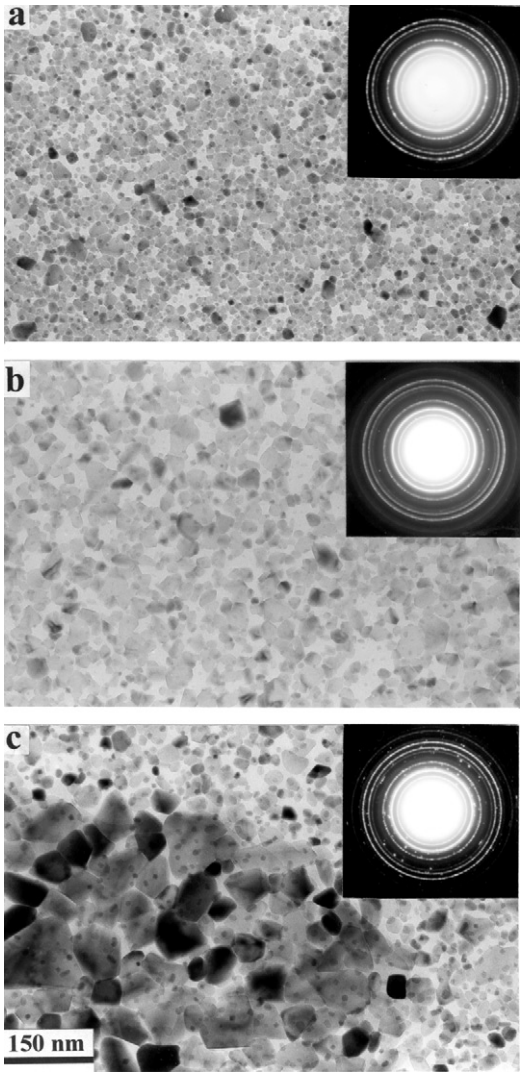

Figure 3. Series of TEM images and SAED patterns (insets) of 4 nm Co/SiO_2 after heating in air for 2 h at: (a) 1073, (b) 1173 and (c) 1273 K.

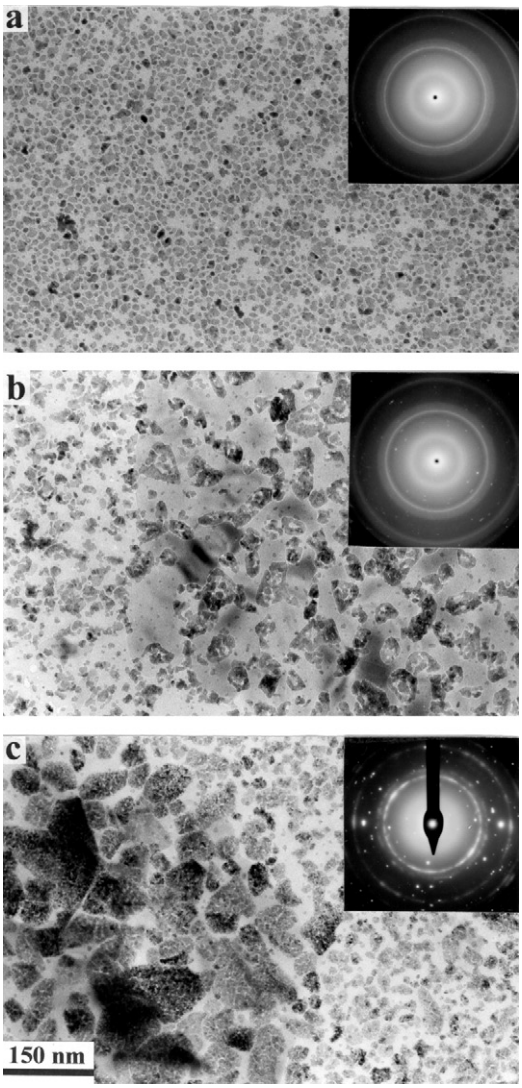

Figure 4. Series of TEM images and SAED patterns (insets) of 4 nm Co/SiO_2 after heating in hydrogen (573 K, 4 h) following previous oxidation in air for 2 h at: (a) 1073, (b) 1173 and (c) 1273 K.

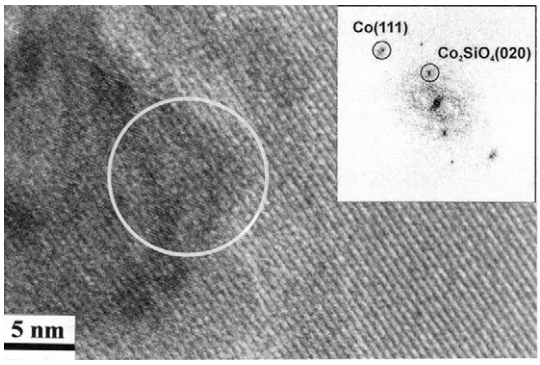

Figure 5. HRTEM image and FFT analysis of marked region of 4 nm Co/SiO_2 after heating at 1173 K in air (2 h) and then at 573 K in hydrogen (4 h).

the SAED patterns (insets) rings of metallic f.c.c. cobalt appeared. However, for the samples previously treated in air at 1173 and 1273 K, additional spots corresponding to cobalt silicate were visible in the SAED patterns, and porous aggregates of crystallites were seen in all regions, including also the specific ones (figure 4).

Analysis of HRTEM images of the samples previously oxidized at 1173 and 1273 K revealed, in specific areas of dark contrast, large crystalline regions with parallel lattice fringes with 0.51, 0.37 and 0.35 nm spacings, which are close to those of the CO_2SiO_4 (020), (101) and (111) planes. Additionally, many small particles with darker contrast are present; some of them exhibit lattice fringes of metallic cobalt. Examples of an HRTEM image and fast Fourier transform (FFT) pattern obtained from the region with dark contrast are shown in figure 5. Spots corresponding to CO_2SiO_4 (020) and Co(111) planes are clearly seen in the FFT pattern. The SAED pattern taken from the large crystalline region (figure 6) could be indexed as cobalt orthosilicate of orientation close to [100].

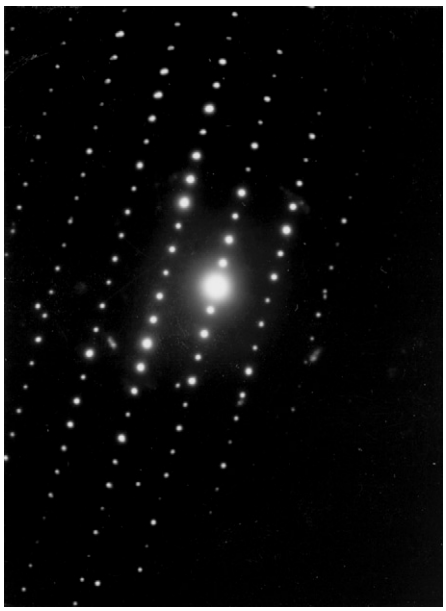

Figure 6. SAED pattern of CO_2SiO_4 crystal in [100] orientation in 4 nm Co/SiO_2 after heating at 1273 K in air (2 h) and then at 573 K in hydrogen (4 h).

4. Discussion

Our investigation of the Co/SiO_2 model system shows that different phenomena determine the structure evolution depending on the cobalt loading. In the sample with low loading spreading of the cobalt phase was observed upon high-temperature treatment in air (at 1173 and 1273 K). With treatment at 1173 K the particle size decreased, while no crystalline phase are observed following heating at 1273 K in air. Since after reduction with hydrogen the crystalline phase reappeared (figures 2(b) and (c)), we assume that the Co phase existed in the oxidized samples in a form undetectable in the TEM images. Similar behavior was observed for other metal supported model systems: Pd/Al_2O_3 [16], Ni/Al_2O_3 [17,18], Ni/SiO_2 [18], Fe/Al_2O_3 [19,20], Pt/Al_2O_3 [21] and Pt/SiO_2 [22]. From these studies and the review of Ruckenstein [23], the complexity of the phenomena should be connected with the chemistry of the metal–support interface. Formed in an oxidizing atmosphere the metal oxide particles have lower surface energy than the metal particles. The formation of the oxide phase resulted in wetting and spreading behavior, whenever heating in hydrogen led to nucleation of particles. For example, marked decrease in the amount of Fe phase present as crystalline particles was observed following heating in oxygen, which reappeared during subsequent reduction [19].

In our investigation the phase obtained after thermal treatment (1273 K, air; 573 K, H_2) could not be identified unambiguously. The rings observed in the SAED patterns (figure 2(c)) with interplanar spacings of 0.24, 0.20, 0.18 and 0.14 nm do not fit metallic Co and may correspond to either Co_3O_4 or cubic CO_2SiO_4 (JCPDF file 15-497). We claim that in this case, the product of the reaction is cubic CO_2SiO_4, which was also established in other work on the $Co–SiO_2$ system after high-temperature treatment [24]. Comparison of the TEM images of the samples subjected to H_2 reduction (figure 2) suggested that more Co phase is present in the sample preheated in air at 1273 than at 1173 K. However, formation of CO_2SiO_4 is accompanied by a three-fold volume increase in relation to Co, which could explain the observed increasing amount of the Co phase. For the sample oxidized at 1073 K, where no spreading occurred, heating in hydrogen caused reduction of the oxide particles to metallic Co and their splitting in accordance with our previous work [25].

In the case of higher-loading model samples, cobalt orthosilicate phase was identified by SAED in addition to Co_3O_4 (insets of figures 3(b) and (c)) after heating at 1173 and 1273 K in air. This silicate phase persisted also in the samples subjected to treatment in hydrogen

at 573 K, while Co_3O_4 was reduced to metallic cobalt (insets of figure 4). The above result is consistent with the literature data [1–13] indicating that the silicate phase is less reducible than Co_3O_4. It seems very likely that porous or/and split aggregates visible on the micrographs (figures 4(b) and (c)) contain Co particles formed upon reduction at 573 K in hydrogen.

In the literature [26] two mechanisms of silicate formation in silica-supported catalysts have been proposed: during the preparation of catalyst, particularly if the pH is alkaline; and as a result of direct solid–solid reaction. The latter takes place during high-temperature treatment [6,9,11]. It is known that at high temperature Co_3O_4 is unstable and decomposes to CoO at 1173–1223 K [27]. From the binary phase diagram of CoO–SiO_2, cobalt orthosilicate forms at temperatures higher than 1173 K [28]. We assume that at high temperature (1173, 1273 K) in air CoO species are present in our sample and they spread over the SiO_2 support. The spreading was clearly observed in this study for the low-loading sample, since no crystalline phase remained (figure 1(c)). Some spreading of CoO occurred also in the high-loading sample but it is masked by the presence of a large amount of crystalline Co oxide. However, for the samples oxidized at high temperature, large flat crystallites of Co silicate are seen in both TEM images and SAED patterns (figures 3(b), 3(c) and 6). It can be expected that spreading of the oxide phase facilitates the reaction with the support. As seen in the micrographs (figures 3 and 4), orthosilicate formed patches, probably because of the heterogeneity of the surface of the support. In HRTEM images of such patches of the reduced sample (figure 5) fringes corresponding to cobalt orthosilicate planes and another small crystalline area assigned to cobalt were observed. We believe that similar morphology appears also in the calcined samples, where Co oxide particles are placed on top of the silicate patches. We cannot deduce unambiguously the spatial arrangement of these two phases from TEM images because they represent the projection of the structure. We suppose, however, that the silicate is formed at the interface between cobalt oxide and silica. Such an arrangement of cobalt and silicate, i.e. cobalt particles on top of the silicate layer, was suggested previously [5,10]. Puskas *et al.* [5] indicated that the reduction of cobalt silicate on high-surface-area silicas requires high temperature (933–1073 K), while for a catalyst with diatomaceous earth reduction occurred in the 773–973 K range. The authors suggest that reduction of the temperature may be possibly due to the hydrogen spillover from cobalt present on the silicate.

As it appears from figure 3(c)), sintering of cobalt oxide is accelerated in the silicate regions. It seems that smooth crystalline silicate plates facilitate particle migration, which is in accordance with a suggestion of Gunter *et al.* [29]. On the other hand, it has been reported that silicate species reduces the sintering of Co in high-surface-area Co/SiO_2 catalysts [7]. We believe that differences in the microstructure and morphology of the silicate phase in such structurally distinct systems could explain this apparent discrepancy.

We observed in this work that Co_3O_4 particles with mean sizes of 13.5, 14.8 and 23 nm were easily reduced to metal in H_2 at 573 K, whereas our recent study on unsupported model samples containing Co_3O_4 particles with comparable mean sizes of 12.1 and 20.3 nm revealed only partial reduction to metallic Co and different morphology of the reduced phase [30]. We suppose that during oxidation of Co supported on SiO_2 considerable strain is generated, especially in case of strong interaction between the particles and the support. It may be expected that reduction of cobalt oxide is easier in the strain region and splitting of the crystallites occurs.

In summary, we can state that the spreading of Co phase was dominant in the low-loading sample (1 nm) after treatment in air at high temperature (1173, 1273 K). In the high-loading sample (4 nm) cobalt orthosilicate was formed as two-dimensional crystalline flakes. We observed that the evolution of the microstructure of Co_3O_4 particles supported on SiO_2 upon reduction differs from that for unsupported ones.

Acknowledgments

The authors thank Dr. L. Kępiński for helpful discussion and critical reading of the manuscript. Thanks are due to Mrs. A. Cielecka and Z. Mazurkiewicz for skilful technical assistance.

References

[1] H.F.J. van't Blik, D.C. Koningsberger and R. Prins, J. Catal. 97 (1986) 210.
[2] G.M. Roe, M.J. Ridd, K.J. Cavell and F.P. Larkins, in: *Methane Conversion,* Studies in Surface Science and Catalysis, Vol. 36, eds. D.M. Biddy, C.D. Chang, R.F. Howe and S. Yurchak (Elsevier, Amsterdam, 1988) p. 509.
[3] M.P. Rosynek and C.A. Polansky, Appl. Catal. 73 (1991) 97.
[4] Y. Okamoto, K. Nagata, T. Adachi, K. Imanaka, K. Inamura and T. Takyu, J. Phys. Chem. 95 (1991) 310.
[5] I. Puskas, T.H. Fleisch, J.B. Hall, B.L. Meyers and R.T. Roginski, J. Catal. 134 (1992) 615.
[6] H. Ming and B.G. Baker, Appl. Catal. A 123 (1995) 23.
[7] K.E. Coulter and A.G. Sault, J. Catal. 154 (1995) 56.
[8] G.J. Haddad and J.G. Goodwin, J. Catal. 157 (1995) 25.
[9] E.V. Steen, G.S. Sewell, R.A. Makhothe, C. Micklethwaite, H. Manstein, M. de Lange and C.T. O'Connor, J. Catal. 162 (1996) 220.
[10] L.B. Backman, A. Rautiainen, A.O.I. Krause and M. Lindblad, Catal. Today 43 (1998) 11.
[11] J.M. Jabłoński, M. Wołcyrz and L. Krajczyk, J. Catal. 173 (1998) 530.
[12] A. Khodakov, O. Ducreux, J. Lynch, B. Rebours and P. Chaumette, Oil Gas Sci. Tech. Rev. IFP 54 (1999) 525.
[13] R.C. Reuel and C.H. Bartholomew, J. Catal. 85 (1984) 63.
[14] J.M. Jabłoński (to be published).
[15] L. Kepinski, Carbon 30 (1992) 949.
[16] E. Ruckenstein and J.J. Chen, J. Catal. 70 (1981) 233.

[17] E. Ruckenstein and S.H. Lee, J. Catal. 86 (1984) 457.
[18] T. Nakayama, M. Arai and Y. Nishiyama, J. Catal. 87 (1984) 108.
[19] I. Sushumna and E. Ruckenstein, J. Catal. 94 (1984) 239.
[20] E. Ruckenstein and I. Sushumna, J. Catal. 97 (1986) 1.
[21] I. Sushumna and E. Ruckenstein, J. Catal. 108 (1987) 77.
[22] R. Lamber and W. Romanowski, J. Catal. 105 (1987) 213.
[23] E. Ruckenstein, in: *Metal–Support Interaction in Catalysis, Sintering and Redispersion*, eds. S.A. Stevenson, J.A. Dumesic, R.T.K. Baker and E. Ruckenstein (Van Nostrand Reinhold, New York, 1987) p. 141.
[24] T. Nguyen, H.L. Ho, D.E. Kotecki and T.D. Nguyen, J. Appl. Phys. 79 (1996) 1123.
[25] D. Potoczna-Petru and L. Kępiński, Catal. Lett. 9 (1991) 355.
[26] J.R. Anderson, *Structure of Metallic Catalyst* (Academic Press, London, 1975) p. 207.
[27] R.C. Weast, M.J. Astle and W.H. Beyer (eds.), *CRC Handbook of Chemistry and Physics*, 69th edition (CRC Press, Boca Raton, FL, 1988–89) p. B-87.
[28] D.P. Mosse and A. Muan, Trans. AIME 233 (1965) 1448.
[29] P.L.J. Gunter, J.W. Niemantsverdriet, F.H. Ribeiro and G.A. Somorjai, Catal. Rev. Sci. Eng. 39 (1997) 131.
[30] D. Potoczna-Petru and L. Kępiński, Catal. Lett. 73 (2001) 41.